Experimental and Theoretical Investigation of Single Cu, Ag, and Au Atoms Adsorbed on Si(111)-(7×7)

Chun Zhang,[1] Gang Chen,[2,1] Kedong Wang,[1] Hongwei Yang,[1] Tao Su,[1] C. T. Chan,[1] M. M. T. Loy,[1] and Xudong Xiao[1,*]

[1]*Department of Physics and Institute of Nano Science and Technology, Hong Kong University of Science and Technology, Hong Kong, China*

[2]*Interdisciplinary Center of Theoretical Studies, Chinese Academy of Sciences, Beijing, China*

(Received 8 September 2004; revised manuscript received 3 January 2005; published 5 May 2005)

Using scanning tunneling microscopy and first principles calculations, the adsorption sites of single Cu, Ag, and Au atoms on the Si(111)-(7 × 7) surface have been systematically investigated and identified. Despite their monovalence, these atoms were found to adsorb at high coordination sites, seeking to saturate the maximum number of dangling bonds. The stable adsorption sites were further observed to be distinctly different in the faulted and unfaulted half unit cells, showing an asymmetry that has never been observed for many other adsorbates.

DOI: 10.1103/PhysRevLett.94.176104 PACS numbers: 68.43.Jk, 68.37.Ef, 68.43.Fg, 68.47.Fg

Silver and gold are two frequently used metallic elements to form electrodes on semiconductor surfaces [1]. Based on a concept of "local softness" for surface reactivity, Brommer *et al.* [2] predicted from their first principles calculations results of a clean Si(111)-(7 × 7) surface that nucleophilic species (e.g., Ag), relative to a Si atom, should react with Si-dangling bonds in the order of adatoms-corner holes-rest atoms, while for electrophilic species (e.g., Au) the order should be corner holes-rest atoms-adatoms. Such conclusions are consistent with chemical intuition that monovalent adsorbates should saturate dangling bonds at semiconductor surfaces [1]. For the well accepted structures of Si(111):Ag-($\sqrt{3} \times \sqrt{3}$)$R30°$ and Si(111):Ag-(3 × 1), the expectation with each Ag atom facing a surface Si-dangling bond for covalent bonds formation appears to hold [1,3,4]. However, from previous experimental studies the adsorption sites and the nature of the bonds between these metallic atoms and Si(111)-(7 × 7) surface remain elusive [5–9].

Scanning tunneling microscopy (STM) is a powerful tool in surface study. While it is often used to observe the adsorption of metallic atoms, the identification of adsorption sites remains nontrivial since STM only measures the local density of states near the Fermi level rather than the metallic atoms themselves [10]. Previous STM studies showed that at low coverage both Ag and Au form similar triangular patterns on Si(111)-(7 × 7) at room temperature [6–9]. While the triangular STM image for Ag was identified as due to a single Ag atom by correlating to the quantitative Ag dosage [6,7], the triangular STM image for Au was speculated as due to a cluster of three Au atoms, each adsorbing at a rest Si atom site within the half unit cell [9].

In this Letter, we report experimental and theoretical investigations on the adsorption sites of Cu, Ag, and Au on Si(111)-(7 × 7). The combination of first principles calculations and STM imaging is found essential for identifying the adsorption sites despite the fact that adsorbates are metallic atoms.

The experiments were carried out with an Omicron low temperature STM in ultrahigh vacuum ($\sim 7 \times 10^{-11}$ torr), with chemically etched tungsten STM tips. The Si(111) wafer was *n* type with a resistivity of 5×10^{-3} to 7 Ω · cm. A small amount of Cu, Ag, or Au, ~0.002 monolayer, was deposited on the clean Si(111)-(7 × 7) surfaces at room temperature. To minimize the STM tip effect, we operated the STM at 50 pA with various bias voltages, which ensured a tip-surface distance of ~8–10 Å as judged from the tunneling current versus tip-surface distance curves.

Figure 1(a) shows the room temperature (RT) STM image of Ag atoms on Si(111)-(7 × 7). As usual, the Si adatoms of the substrate appear bright, showing the

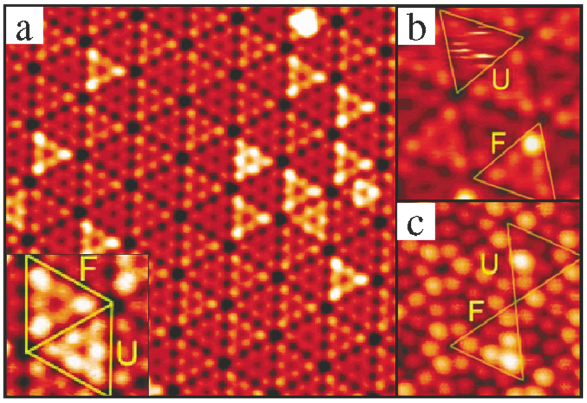

FIG. 1 (color). Topographic STM images of Ag on Si(111)-(7 × 7) at (a) 298, (b) 78, and (c) 5 K. The tunneling current and sample bias are set at 50 pA and −2 V, respectively. The fuzzy image in UHUC at 78 K is due to the nonfrozen motion of Ag. The inset in (a) gives typical images of single Ag in FHUC and UHUC, respectively, showing brightness contrast between the corner and center spots.

brighter faulted half unit cell (FHUC) and the dimmer unfaulted half unit cell (UHUC), respectively [11]. The triangular patterns, each with six bright spots, three at the corners and three at the centers, observed at RT can be seen to originate from a single Ag atom hopping frequently from site to site within the half unit cell. As we will see later, each bright spot here is correlated with, but does not necessarily represent, the Ag adsorption site. When the sample temperature was lowered to 78 K [Fig. 1(b)], single bright spots at the *corner* Si adatom sites were imaged for single Ag atoms in the FHUC. At 5 K [Fig. 1(c)], the Ag atoms in the UHUC also ceased hopping and bright spots at the *center* Si adatom sites were imaged instead. This change in STM images between room temperature and low temperature is found reversible. The less frequent observation of the bright spot at the center Si adatom sites in the FHUC and at the corner Si adatom sites in the UHUC at low temperatures indicates that their corresponding Ag adsorption sites are metastable. This is consistent with the room temperature images [see inset of Fig. 1(a)] where the brightness of the spots represents the relative amount of residence time and thus the relative stability for their corresponding Ag adsorption sites. To our best knowledge, this is the first time that distinctively different stable adsorption sites on the two half unit cells have been observed on Si(111)-(7 × 7). By analyzing the resident times t at a given temperature T [12], we obtain an estimate of the difference in binding energies E between the stable and metastable sites from the relation $t \propto \exp(-E/kT)$. The results are shown in Table I.

The behavior of Cu and Au atoms adsorbed on this surface, in terms of the bright spot positions and the FHUC/UHUC asymmetry, is found *identical* to Ag, both at room and low temperatures. This already deviates from the bonding model proposed by Brommer *et al.* [2], who suggested that Ag and Au would preferentially adsorb at corner Si adatom and Si rest atom sites, respectively.

At first sight, the STM images at low temperatures might appear to support the notion that Si adatoms are the adsorption sites for these three elements. However, whether the bright spot in fact represents the adsorption site requires theoretical calculations [10], for which we have performed first principles calculations [13,14] within the framework of density functional theory (DFT). We employed the projector augmented-wave (PAW) method [15] and the exchange correlation with the generalized gradient approximation by the Perdew, Burke, and Ernzerhof (PBE-GGA) [16]. A repeated-slab geometry is used, with six Si layers separated by a 12 Å vacuum. The unit cell has 298 Si atoms and 49 H atoms to terminate the bottom Si layer. The wave functions are expanded in a plane wave basis with an energy cutoff of 250 eV for Ag and Au, and 370 eV for Cu; only the Γ point is used in the summation of the Brillouin zone of the simulation cell. The Si atoms on the bottom layer are fixed and all the other atoms are fully relaxed until the forces are less than 5 meV/Å for the stable and metastable absorption sites and 20 meV/Å for other sites.

TABLE I. The experimental and theoretical binding energy difference between the metastable and stable adsorption sites on FHUC and UHUC for Cu, Ag, and Au. The last column is the calculated binding energy difference between the stable adsorption sites in FHUC and UHUC. The experimental error is 5 meV and the calculation error is 20 meV.

Atom	$E_{S'} - E_S$ (meV), FHUC		$E_S - E_{S'}$ (meV), UHUC		$E(F) - E(U)$ (meV)
	Exp.	Cal.	Exp.	Cal.	Cal.
Cu	50	−20	30	60	−40
Ag	>80	10	5	50	−40
Au	30	~0	30	50	−10

Figures 2(a) and 2(b) show the calculated binding energy for a number of selected sites both in FHUC and UHUC for Cu, Ag, and Au, together with K. The binding energy is operationally defined as the energy difference between the fully relaxed system and that with the metal atoms pulled up 8 Å into the vacuum, with the substrate relaxed. The sites are labeled with respect to the dimer-adatom-stacking fault (DAS) model [17]. By symmetry, we need only to consider one of the three equivalent "basins" [18,19] defined by the central Si rest atom and three surrounding Si adatoms [Fig. 2(c)]. Our results indicate that the dangling bond Si rest atom and the Si adatom, either at the corner or at the center, are *not* the adsorption sites because their binding energies are ~0.8–1.7 eV higher than the respective lowest energy sites, in strong contrast to the experimentally observed bright spot positions. With a full relaxation, we found that the lowest energy sites are the S (S') sites for FHUC (UHUC), which is laterally close to the B_2 (B_2') sites but has a lower symmetry. The decrease of the overall binding strength in

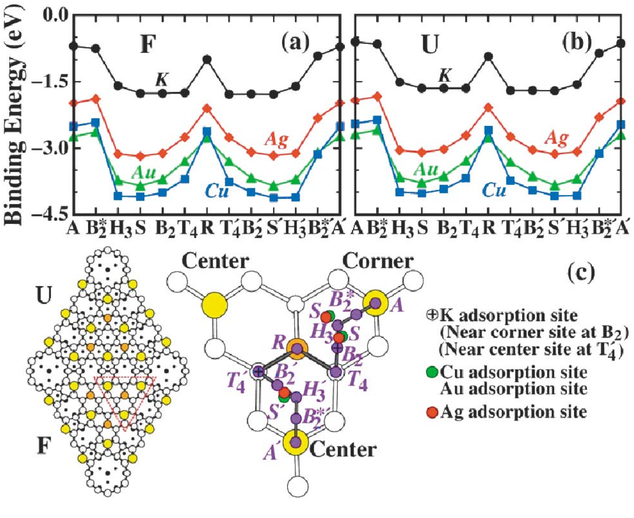

FIG. 2 (color). The binding energy obtained from first principles calculations for K, Cu, Ag, and Au at selected sites in FHUC (a) and UHUC (b). (c) The DAS model and the basin on which the selected sites are labeled.

the order of Cu > Au > Ag is due to the decreasing hybridization between the *d* electrons and the surface. K has no *d* electron contribution and thus has the weakest binding energy of all. The binding energy difference for Cu, Ag, and Au at the stable and metastable adsorption sites in both FHUC and UHUC is listed in Table I to compare with the experimental values. The somewhat stronger binding in the FHUC is consistent with the preferential occupation of Ag, Au, and Cu in the FHUC at thermal equilibrium as observed in our experiment and also in other adsorbate systems [5,20,21].

The above conclusion can be directly compared to a recent first principles study by Cho and Kaxiras [18,19] for K, Mg, Ga, Si, and Ge, using a (4×4) supercell rather than a full (7×7) cell. They found that for all adsorbates the dangling bond sites are unstable. The lowest energy sites are the T_4-type (for K and Ga), H_3-type (for Mg), or B_2-type (for Si and Ge) sites. Our calculation with full relaxation for K on the full (7×7) unit cell reproduced their results. Full (7×7) unit cell calculations for Na [22], Si [23], and Pb [24] also reached a similar conclusion. While it is not surprising that multivalent elements would like to saturate their orbitals by adsorbing at high coordination sites, it is not obvious why monovalent atoms, in particular, Ag and Cu with similar electronegativity as Si [1,25], would adsorb at the high coordination sites instead of saturating the dangling bonds.

Potassium, with its low electronegativity [1,25], forms ionic bonds with Si(111) by transferring its *s* electron to the surface, as is visually evident from charge density difference plots. It is thus not surprising that K prefers high coordination site adsorption. For Cu and Ag, however, there is no obvious charge transfer between the adsorbates and the surface, judging from the charge density difference plots in addition to their comparable electronegativity as Si [1,25]. Thus, their bindings to Si surface should not be attributed to the ionic bond. To understand why these monovalent adsorbates prefer high coordination adsorption sites, we plot in Fig. 3, as an example, the isosurface of charge density and the charge density contours along the Ag-Si bonds for Ag adsorbed both at the *S* site and at the corner Si adatom dangling bond site in the FHUC. We see that the charge densities between Ag at the *S* site and the nearest three Si atoms (the corner Si adatom Si1, Si rest atom Si2, and another neighbor Si atom Si3) are somewhat smaller but still *comparable* to that for an Ag atom adsorbing at a top site of the corner Si adatom. From Fig. 2, the binding energy for Ag saturating one single Si-dangling bond is ~ -2.0 eV. However, forming three bonds between the Ag atom at the *S* site and three neighboring Si atoms, although each one is weaker, the binding energy becomes more favorable (~ -3.1 eV) than saturating one single dangling bond. Thus, for these relatively large size metallic elements (Cu, Ag, and Au) with an essentially complete *d* shell so that they are "spherical" and have no preferred bond angles, they can interact with multiple Si surface atoms by occupying a higher coordinated site and thus saturate the maximum number of dangling bonds on the surface. The situation is different for atoms such as H, which is very small in size and can bond with only one Si atom [Figs. 3(c) and 3(f)].

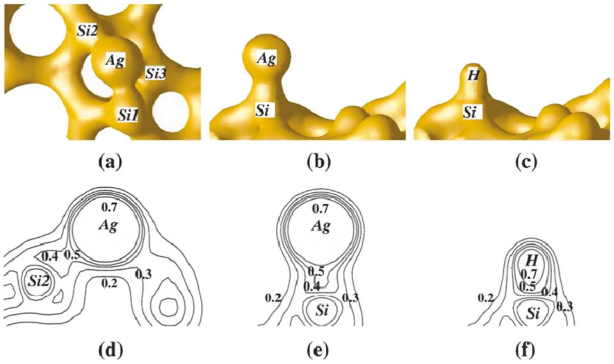

FIG. 3 (color). The isosurfaces of charge density at $0.3e/\text{Å}^3$ plotted for (a) Ag at *S* site (top view), (b) Ag, and (c) H at corner Si adatom site (side view) in FHUC. (d)–(f) are the corresponding charge density contours in the cross section of the bonds ($e/\text{Å}^3$).

Now, we have to address the apparent different positions between the calculated most favorable adsorption site (*S* or *S'*) and the experimental bright spot, which almost coincides with the Si adatom site from -3 to $+1$ V and moves a little beyond the H_3 site above $+2$ V, in contrast to many other adsorbates such as H [26,27], Si [23,28], and Pb [24] for which no strong bias dependence was found. By placing the atoms at the lowest energy site, we can simulate the STM images from first principles calculations using the model of Tersoff and Hamann [29]. In Fig. 4, we show the simulation results together with the experimental images at 77 K for Ag in the FHUC at several biases. We have superimposed the two simulated images with the Ag atom sitting on either of the two equivalent *S* sites near the corner Si adatom [Fig. 2(c)]. Because of the very low barrier (~50 meV) between them that allows frequent hopping, the experiment image is actually the superposition of images of the two equivalent sites. The agreement between experiment and theory is quite satisfactory, with the bright spot more or less reproduced by the simulation at different biases. Simulations with Ag at the *S'* site in

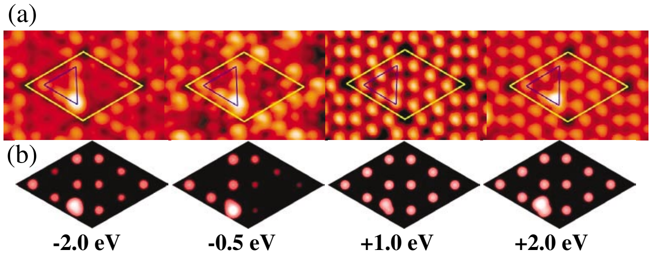

FIG. 4 (color). (a) STM images of a single Ag atom in the faulted Si(111)-(7×7) half unit cell at 77 K for a number of sample biases. (b) The simulated STM images, with the charge density calculated at 3 Å above the Ag adatom.

FHUC would cause the center Si adatom to be bright at negative bias and show similar bias dependence behavior as the S site. Since the binding energy at the H_3 and B_2 sites is about 50 and 60 meV, respectively, higher than that at the S site, adsorption at H_3 and B_2 is also possible at finite temperature. In this regard, STM image simulations indicate an agreement with experiment for the H_3 site but not for the B_2 site adsorption. Similar conclusions can be made for Ag in the UHUC except with different stability. The bias dependence of the bright spot position is caused by electronic effects since at negative bias (and small positive bias) the image is overwhelmingly dominated by electronic states (not charge transfer) near the Fermi level of the corner Si adatom, and only at high positive bias the unoccupied s state of the Ag atom starts to compete with those of Si. The vertical rise of 0.35–0.40 Å for the corner Si adatom near the adsorbed Ag, induced by the proximity of the adsorbed Ag, also contributes to its brightness. The pictures for Cu and Au are similar. Thus, by combining first principles calculations and STM experiment, we can conclude that Ag, Cu, and Au atoms all adsorb at high coordination sites rather than the Si-dangling bond sites as proposed earlier [1,2].

While we can reconcile the theoretical adsorption site with the experimentally observed bright STM spot, the calculation could not fully reproduce the stability of different adsorption sites in the two halves. As shown in Table I, while in experiment we have consistently observed a preferred adsorption near the corner Si adatom (S site) in the FHUC and near the center Si adatom (S' site) in the UHUC for all three elements, the calculations, however, underestimate the binding energy difference in the FHUC but overestimate the difference in the UHUC. For the case of Cu in FHUC, the sign is wrong. Further refined calculation, for example, using more k points in the Brillouin zone, may help to identify the discrepancy [30]. We of course recognize that the GGA formulation is not exact.

In summary, with STM imaging and density functional calculations, we have clearly identified high coordination sites as the adsorption sites for single Cu, Ag, and Au atoms on $\mathrm{Si}(111)-(7\times 7)$ surface. While the bright spot is nearly on top of the Si adatom sites at most bias voltages, theoretical calculations show that the Si-dangling bonds are unfavorable for adsorption for any of these elements, in contrast to common belief. Electronic effect was found important to reconcile the apparent different positions between the bright STM image spot and the stable adsorption site. Experimentally, the stable adsorption sites were further found different for the two half unit cells, showing an observable asymmetry.

This work was supported by HKUST Research Infrastructure and the Research Grants Council of Hong Kong (RGC 604504 and HKUST6152/01P). G. C. was also partially supported by the China Postdoctoral Science Foundation. Computing resources are supported by HIA grants at HKUST, and we also thank ITP and ICTS, CAS for the generous allocation of computer time on the HP-SC45 Sigma-X computer.

---

*Corresponding author.
Email: phxudong@ust.hk

[1] W. Mönch, *Semiconductor Surfaces and Interfaces* (Springer, New York, 2001), and references therein.
[2] K. D. Brommer *et al.*, Surf. Sci. **314**, 57 (1994).
[3] S. Kono, K. Higashiyama, and T. Sagawa, Surf. Sci. **165**, 21 (1986).
[4] C. Collazo-Davila, D. Grozea, and L. D. Marks, Phys. Rev. Lett. **80**, 1678 (1998).
[5] St. Tosch and H. Neddermeyer, Phys. Rev. Lett. **61**, 349 (1988).
[6] H. Hirayama, H. Okamoto, and K. Takayanagi, Phys. Rev. B **60**, 14260 (1999).
[7] T. Jarolímek *et al.*, Surf. Sci. **482**, 386 (2001).
[8] P. Sobotík, P. Kocán, and I. Ošt'ádal, Surf. Sci. **537**, L442 (2003).
[9] I. Chizhov, G. Lee, and R. F. Willis, Appl. Phys. A **66**, S1003 (1998).
[10] C. J. Chen, *Introduction to Scanning Tunneling Microscopy* (Oxford University Press, New York, 1993).
[11] R. M. Trump, R. J. Hamers, and J. E. Demuth, Phys. Rev. B **34**, 1388 (1986).
[12] K. D. Wang *et al.*, Phys. Rev. Lett. **94**, 036103 (2005).
[13] Calculations were performed using the VASP package. See, for example, G. Kresse and J. Hafner, Phys. Rev. B **47**, 558 (1993); **49**, 14251 (1994); G. Kresse and J. Furthmüller, Comput. Mater. Sci. **6**, 15 (1996).
[14] G. Kresse and J. Furthmüller, Phys. Rev. B **54**, 11 169 (1996); G. Kresse and D. Joubert, Phys. Rev. B **59**, 1758 (1999).
[15] P. E. Blöchl, Phys. Rev. B **50**, 17 953 (1994).
[16] J. P. Perdew, K. Burke, and M. Ernzerhof, Phys. Rev. Lett. **77**, 3865 (1996).
[17] K. Takayanagi *et al.*, Surf. Sci. **164**, 367 (1985).
[18] K. Cho and E. Kaxiras, Europhys. Lett. **39**, 287 (1997).
[19] K. Cho and E. Kaxiras, Surf. Sci. **396**, L261 (1998).
[20] M. Y. Lai and Y. L. Wang, Phys. Rev. Lett. **81**, 164 (1998).
[21] L. Vitali, M. G. Ramsey, and F. P. Netzer, Phys. Rev. Lett. **83**, 316 (1999).
[22] K. Wu *et al.*, Phys. Rev. Lett. **91**, 126101 (2003).
[23] C. M. Chang and C. M. Wei, Phys. Rev. B **67**, 033309 (2003).
[24] O. Custance *et al.*, Phys. Rev. B **67**, 235410 (2003).
[25] *Handbook of Chemistry and Physics*, edited by D. R. Lide (CRC Press, New York, 2001).
[26] R.-L. Lo *et al.*, Phys. Rev. Lett. **80**, 5584 (1998).
[27] A. Vittadini and A. Selloni, Phys. Rev. Lett. **75**, 4756 (1995).
[28] T. Sato, S. Kitamura, and M. Iwatsuki, J. Vac. Sci. Technol. A **18**, 960 (2000).
[29] J. Tersoff and D. R. Hamann, Phys. Rev. Lett. **50**, 1998 (1983).
[30] G. Makov, R. Shah, and M. C. Payne, Phys. Rev. B **53**, 15513 (1996).